B-spline *R*-matrix-with-pseudostates calculations for electron-impact excitation and ionization of nitrogen

Yang Wang,[1,*] Oleg Zatsarinny,[2,†] and Klaus Bartschat[2,3,‡]

[1]*Center for Theoretical Atomic and Molecular Physics, Academy of Fundamental and Interdisciplinary Sciences, Harbin Institute of Technology, Harbin 150080, People's Republic of China*

[2]*Department of Physics and Astronomy, Drake University, Des Moines, Iowa 50311, USA*

[3]*ARC Centre for Antimatter-Matter Studies, School of Chemical and Physical Sciences, Flinders University, GPO Box 2100, Adelaide, SA 5001, Australia*

(Received 9 May 2014; published 23 June 2014)

The *B*-spline *R*-matrix-with-pseudostates (BSR) method is employed to treat electron collisions with nitrogen atoms. Predictions for elastic scattering, excitation, and ionization are presented for all transitions between the lowest 21 states of nitrogen in the energy range from threshold to 120 eV. The structure description has been further improved compared to a previous BSR calculation by Tayal and Zatsarinny [J. Phys. B **38**, 3631 (2005)]. This change in the structure model, together with the inclusion of a large number of pseudostates in the close-coupling expansion, has a major influence on the theoretical predictions, especially at intermediate energies, where many of the excitation cross sections are reduced significantly. Ionization cross sections for the ground and metastable initial states are also provided. Finally, we carry out an accurate *ab initio* treatment of the prominent shape resonance just above the elastic threshold.

DOI: 10.1103/PhysRevA.89.062714 PACS number(s): 34.80.Bm, 34.80.Dp

I. INTRODUCTION

Accurate atomic data for electron collisions with nitrogen atoms are of importance in the modeling of different plasmas. Many strong emission lines of nitrogen are observed in the atmosphere of the Sun and a variety of other astrophysical objects. The intensity ratios of these lines are used for temperature and density diagnostics in planetary atmospheres and air plasmas, in which, e.g., N_2, NF_3, or NH_3 may break up. To model such plasmas, a variety of *e*-N energy levels, oscillator strengths, and collision cross sections are required [1–3].

One of the intriguing features of electron-nitrogen scattering is a prominent shape resonance located very close to the elastic threshold. No stable negative-ion state of nitrogen has yet been observed, and numerous scattering calculations have suggested that the lowest $N^-(2s^22p^4)^3P$ feature is, in fact, a low-energy resonance at an energy less than 0.2 eV above the ground state of nitrogen. This resonance dominates the low-energy regime and completely defines the shape and magnitude of the elastic cross section. Experimental evidence for the ^3P shape resonance comes from electron-energy-loss spectroscopy of N_2 and NO by Mazeau *et al.* [4]. They suggest a value of $E(N^-\,^3P) - E(N\,^4S^o) = 70 \pm 20$ meV with a width of 16 ± 5 meV. Although an early calculation by Burke *et al.* [5] predicted the $N^-\,^3P$ resonance to lie within 0.1 eV of the experimental value, a more extensive calculation by the same group [6] subsequently shifted the resonance position to a bound state below the elastic threshold. This is an indication that those calculations were not fully converged with respect to the target states retained in the close-coupling expansion. Another attempt of an *ab initio* description of the ^3P resonance was undertaken by Ramsbottom and Bell [7]. They, too, failed to produce a low-energy ^3P resonance feature and hence used a semi-empirical shift of the relevant *R*-matrix poles to obtain the resonance position in accordance with the measurements [4]. Consequently, there clearly exists a significant uncertainty regarding elastic *e*-N scattering below 1 eV.

The available experimental data for excitation of atomic nitrogen by electron impact are very scarce. Absolute angle-differential and angle-integrated excitation cross sections were reported by Doering and Goembel for the $(2p^23s)^4P$ state [8] and later for the $(2s2p^4)^4P$ state [9] at incident-electron energies of 30, 50, and 100 eV. Subsequently, Yang and Doering [10] reported excitation cross sections for the forbidden $(2s^22p^3)^4S^o$-$^2D^o$ transition at incident-electron energies between 5 and 30 eV. A detailed theoretical description of this forbidden transition was provided by Tayal and Beatty [11]. They employed the *R*-matrix method in an 11-state close-coupling approximation and obtained very good agreement with the other available calculations at the time and also the measurements.

More extensive calculations were presented by Tayal and Zatsarinny [12], who reported excitation cross sections for a set of forbidden and resonance transitions in atomic nitrogen for incident-electron energies from threshold to 120 eV. Their close-coupling expansion included 24 spectroscopic bound and autoionizing states together with 15 pseudostates. The latter were chosen to approximate the loss of flux into the infinite number of bound and continuum target states that are dipole coupled to terms with the ground-state configuration. Already then a significant effect of the ionization continuum was found on the theoretical predictions for the resonance transitions. The limited number of pseudostates, however, did not allow for a thorough assessment of the quality of the calculated cross sections.

The electron-impact ionization cross section for atomic nitrogen was measured by Brook *et al.* [13] over a wide range

*yangwang0624@foxmail.com
†oleg.zatsarinny@drake.edu
‡klaus.bartschat@drake.edu

of energies from threshold to 1000 eV. These measurements were analyzed by Kim and Desclaux [14] within the binary encounter Bethe (BEB) approach. While very successful in many cases, the BEB calculation predicted 25% lower ionization cross sections in the nitrogen case than the experimental values. To explain the difference, Kim and Desclaux suggested a large population of metastable states (up to 30%) that seems unrealistic.

The purpose of the present paper, therefore, is to extend the previous calculations [12] and thereby provide an additional assessment for the likely accuracy of the available collision data. As shown in our recent work on e-Ne [15,16] and e-C collisions [17], coupling to the ionization continuum and, albeit to a smaller extent, the higher-lying discrete Rydberg spectrum as well as autoionizing states, can have a major effect on theoretical predictions for electron-induced transitions including both optically allowed and optically forbidden transitions. It seemed highly appropriate to carry out much larger calculations than were possible just a few years ago and thereby to provide a complete (for the purpose of most modeling applications) and consistent set of scattering data that includes elastic-scattering, excitation, and ionization processes.

In recent years, we have extended the B-spline R-matrix (BSR) code [18] in several ways, with the most important development for the present case of interest being the ability to include a large number of pseudostates in the close-coupling expansion. As in the convergent close-coupling (CCC) [19] and standard R-matrix-with-pseudostates (RMPS) [20] approaches, these states are of finite range and hence represent discrete-level approximations of the high-lying Rydberg spectrum and the ionization continuum. While the coupling to these infinite manifolds cannot be accounted for exactly, the pseudostates provide a sufficiently accurate representation of the basic effect, and as an additional benefit they even allow for the calculation of ionization processes. More recent examples using the BSR code for ionization and even ionization with simultaneous excitation of helium can be found in Refs. [21,22].

The particular advantages of our BSR implementation are: (i) While the current CCC program is limited to the treatment of the valence electron(s) in quasi-one- and quasi-two-electron systems, the BSR suite of codes is a general package that can be applied to complex open-shell targets. (ii) Compared to the well-known and frequently used Belfast suite of R-matrix codes [23,24], the BSR approach allows for the use of nonorthogonal orbital sets. These orbitals provide a vastly increased flexibility in the target description. Although the price to pay is a significant increase in the complexity of setting up the Hamiltonian matrix and, consequently, the computational resources required, the reward of a much-improved target description has in many cases been well worth the effort.

This paper is organized as follows: We begin in Sec. II by summarizing the most important features of the present model for the e-N scattering process. This is followed in Sec. III with a presentation and discussion of our present results, in comparison with those from previous calculations and, in rare cases, experimental data. Besides presenting elastic and momentum-transfer cross sections, results for state-selective excitation processes, and finally electron-impact ionization, we will also combine the results in a form that might be useful for plasma applications. In particular, we will include elastic scattering, the sum of all inelastic excitations, superelastic deexcitation (in case the initial state is not the ground state), and ionization to form the "grand-total cross section." We finish with a brief summary and conclusions in Sec. IV.

II. COMPUTATIONAL DETAILS

A. Structure calculations

The target states of atomic nitrogen in the present calculations were generated by combining the multiconfiguration Hartree–Fock (MCHF) and the B-spline box-based close-coupling methods [25]. Specifically, the structure of the multichannel target expansion was chosen as

$$\begin{aligned}\Phi(2s^2 2p^3 nl, LS) = &\sum_{nl,L'S'} \{\phi(2s^2 2p^2, L'S')P(nl)\}^{LS} \\ &+ \sum_{nl,L'S'} \{\phi(2s2p^3, L'S')P(nl)\}^{LS} \\ &+ a\varphi(2s^2 2p^3)^{LS} + b\varphi(2s2p^4)^{LS}. \quad (1)\end{aligned}$$

Here, $P(nl)$ denotes an orbital of the outer valence electron, while the ϕ and φ functions represent the configuration-interaction (CI) expansions of the corresponding ionic or specific atomic states, respectively. These expansions were generated in separate MCHF calculations for each state using the MCHF program [26].

The expansion (1) can be considered a model for the entire $2s^2 2p^2 nl$ and $2s2p^3 nl$ Rydberg series of bound and autoionizing states in neutral nitrogen, including the continuum pseudostates lying above the ionization limit. The first two sums in this expansion can also provide a good approximation for states with equivalent electrons; namely, for all terms of the ground-state configuration $2s^2 2p^3$ as well as the core-excited $2s2p^4$ states. We found, however, that it is more appropriate to employ separate CI expansions for these states by directly including relaxation and term-dependence effects via state-specific one-electron orbitals.

The inner-core (short-range) correlation is accounted for through the CI expansion of the $2s^2 2p^2$ and $2s2p^3$ ionic states. These expansions include all single and double excitations from the $2s$ and $2p$ orbitals to the $3l$ and $4l$ ($l = 0$–3) correlated orbitals. These orbitals were generated for each state separately. To maintain the final expansions for the atomic states at a reasonable size, all CI expansions were restricted by dropping contributions with coefficients whose magnitude was less than the cutoff parameter of 0.01. The resulting ionization potentials for all ionic states agreed with experiment [27] to within 0.01 eV.

The unknown functions $P(nl)$ for the outer valence electron were expanded in a B-spline basis, and the corresponding equations were solved subject to the condition that the orbitals vanish at the boundary. The R-matrix radius was set to $30a_0$, where $a_0 = 0.529 \times 10^{-10}$ m is the Bohr radius. We employed 84 B-splines of order 8 to span this radial range using a semi-exponential knot grid. The B-spline coefficients for the valence electron orbitals $P(nl)$, along with the coefficients a

TABLE I. Excitation energies (in eV) for the spectroscopic target states of atomic nitrogen. The energy splittings listed by NIST [27] and the differences with the present and the previous BSR calculations [12] are given as well.

				Difference	
	State	Term	NIST	Present	Ref. [12]
1	$2s^2 2p^3$	$^4S^o$	0.000	0.000	0.000
2	$2s^2 2p^3$	$^2D^o$	2.384	0.007	0.074
3	$2s^2 2p^3$	$^2P^o$	3.576	−0.008	0.184
4	$2s^2 2p^2(^3P)3s$	^4P	10.332	0.090	0.212
5	$2s^2 2p^2(^3P)3s$	^2P	10.687	0.087	0.063
6	$2s2p^4$	^4P	10.927	0.021	0.197
7	$2s^2 2p^2(^3P)3p$	$^2S^o$	11.603	0.015	0.031
8	$2s^2 2p^2(^3P)3p$	$^4D^o$	11.758	0.027	0.157
9	$2s^2 2p^2(^3P)3p$	$^4P^o$	11.842	0.029	0.101
10	$2s^2 2p^2(^3P)3p$	$^4S^o$	11.996	0.007	0.067
11	$2s^2 2p^2(^3P)3p$	$^2D^o$	12.006	0.021	0.069
12	$2s^2 2p^2(^3P)3p$	$^2P^o$	12.125	0.020	0.191
13	$2s^2 2p^2(^1D)3s$	^2D	12.357	0.016	0.004
14	$2s^2 2p^2(^3P)4s$	^4P	12.856	−0.003	0.014
15	$2s^2 2p^2(^3P)4s$	^2P	12.919	−0.001	0.007
16	$2s^2 2p^2(^3P)3d$	^2P	12.972	−0.009	0.020
17	$2s^2 2p^2(^3P)3d$	^4F	12.984	−0.013	0.018
18	$2s^2 2p^2(^3P)3d$	^4P	12.999	−0.017	0.035
19	$2s^2 2p^2(^3P)3d$	^2F	13.000	−0.013	0.032
20	$2s^2 2p^2(^3P)3d$	^4D	13.019	−0.014	0.082
21	$2s^2 2p^2(^3P)3d$	^2D	13.035	−0.014	0.281

and b for the perturbers, were obtained by diagonalizing the atomic Hamiltonian in the nonrelativistic LS approximation. Since the B-spline bound-state close-coupling calculations generate different nonorthogonal sets of orbitals for each atomic state, their subsequent use is somewhat complicated. Our configuration expansions for the atomic target states contained up to 250 configurations for each state. These could still be used in the subsequent large-scale collision calculations with our currently available computational resources.

Table I shows a comparison between the calculated spectrum of nitrogen and the values of the multiplets listed in the NIST Atomic Levels and Spectra database [27]. The overall agreement between our results and the latter tables is satisfactory, with the deviations in the energy splitting being less than 30 meV for most states. Larger deviations of up to 90 meV are observed only for the $2p^3 3s$ states. For these states more significant corrections are expected due to a core-valence correlation that was not included to full extent in our limited target BSR expansion (1). A more accurate description of the core-valence correlation effects would require additional ionic states, such as $2s2p^2 3s$ or $2s2p^2 3d$, to describe important $2p$-$3s$ and $2p$-$3d$ promotions. While such an improvement may currently be realistic for structure-only calculations, it would increase the target expansions to a level that we cannot handle yet in the consequent scattering calculations.

The current structure description is superior to that generated by Tayal and Zatsarinny [12], where the wave functions for the target states where generated based on the MCHF method alone. The BSR approach has the advantage that it allows us to generate the entire spectrum with the same accuracy, whereas the MCHF approach is based on optimization of individual levels. Note that expansion (1) also provides the continuum pseudostates used to describe the ionization processes. The number of pseudostates strongly depends on the box size. In order to cover the maximum possible target continuum we chose a relatively small box radius of $30a_0$. This choice, however, restricts the number of spectroscopic target states that can be generated accurately by the method. Table I only lists those states that we consider sufficiently well represented in this scheme.

TABLE II. Oscillator strengths for selected dipole-allowed transitions in atomic nitrogen.

Lower level	Upper level	Ref. [12]	Present	Expt.
$2p^3\ ^4S^o$	$2p^2(^3P)3s\ ^4P$	0.252	0.278	0.271[a]
				0.266[b]
	$2s2p^4\ ^4P$	0.100	0.079	0.078[b]
				0.080[c]
				0.085[d]
	$2p^2(^3P)4s\ ^4P$	0.024	0.033	0.030[c]
				0.027[d]
	$2p^2(^3P)3d\ ^4P$	0.071	0.074	0.067[c]
				0.075[d]
$2p^3\ ^2D^o$	$2p^2(^3P)3s\ ^2P$	0.069	0.068	0.071[d]
	$2p^2(^3P)4s\ ^2P$	0.007	0.012	0.013[b]
	$2p^2(^3P)3d\ ^2P$	0.001	0.001	
	$2p^2(^1D)3s\ ^2D$	0.077	0.075	0.083[d]
	$2p^2(^3P)3d\ ^2D$	0.010	0.006	
	$2p^2(^3P)3d\ ^2F$	0.061	0.033	0.032[b]
	$2s2p^4\ ^2D$		0.058	
$2p^3\ ^2P^o$	$2p^2(^3P)3s\ ^2P$	0.061	0.059	0.061[d]
	$2p^2(^3P)4s\ ^2P$	0.005	0.002	0.003[e]
	$2p^2(^3P)3d\ ^2P$	0.019	0.021	0.020[e]
	$2p^2(^1D)3s\ ^2D$	0.028	0.026	
	$2p^2(^3P)3d\ ^2D$	0.066	0.033	0.037[e]
	$2s2p^4\ ^2D$		0.018	

[a]Ref. [28].
[b]Ref. [29].
[c]Ref. [30].
[d]Ref. [31].
[e]Ref. [32].

Another assessment regarding the quality of our target description can be obtained by comparing the results for the oscillator strengths of various transitions with experimental data and other theoretical predictions. Such a comparison is given in Table II for a set of transitions from the ground and metastable states of nitrogen. In most cases, we see close agreement between our results and the values from different measurements. There is also good agreement with predictions from our previous calculations [12]. In some cases, however, including the transitions $(2p^3)^2D^o$-$(2p^2 3d)^2F$ and $(2p^3)^2P^o$-$(2p^2 3d)^2D$, the present model still provides significant further improvement. We thus conclude that the oscillator strengths for most of these transitions are very well established now, to an accuracy of a few percent. A more detailed comparison with other available data at the time is given in Ref. [12].

Table II also contains the f values for excitation of the $(2s2p^4)^2D$ state, which will be discussed later in connection with ionization. This state lies above the ionization threshold and quickly decays via autoionization. Consequently, its excitation will ultimately contribute to the observed ionization signal.

B. Scattering calculations

Our close-coupling expansion includes 690 states of atomic nitrogen, with 56 states representing the bound spectrum and the remaining 644 representing the target continuum and some core-excited autoionizing states. We included all doublet and quartet target states with total electronic orbital angular momentum $L = 0$–4. The continuum pseudostates in the present calculations cover the energy regime up to 50 eV above the ionization limit. This model will be referred to as BSR-690 below. As a check for the sensitivity of the results regarding coupling to the high-lying Rydberg states as well as the ionization continuum, we also performed a 61-state calculation (labeled BSR-61), which contains the bound and autoionizing states $2s^22p^3$, $2s2p^4$, $2s^22p^23l$, and $2s2p^43l$ with all possible total and intermediate terms. We used the same target description in both the BSR-690 and BSR-61 models.

The close-coupling equations were solved by means of the R-matrix method by using a parallelized version of the BSR complex [18]. The distinctive feature of the method is the use of B splines as a universal basis to represent the scattering orbitals in the inner region of $r \leqslant a$. Hence, the R-matrix expansion in this region takes the form

$$\Psi_k(x_1,\ldots,x_{N+1}) = \mathcal{A}\sum_{ij}\bar{\Phi}_i(x_1,\ldots,x_N;\hat{\mathbf{r}}_{N+1}\sigma_{N+1})r_{N+1}^{-1}B_j(r_{N+1})a_{ijk} + \sum_i \chi_i(x_1,\ldots,x_{N+1})b_{ik}. \quad (2)$$

Here, the $\bar{\Phi}_i$ denote the channel functions constructed from the N-electron target states and the angular and spin coordinates of the projectile, while the splines $B_j(r)$ represent the radial part of the continuum orbitals. The χ_i are additional $(N+1)$-electron bound states. In standard R-matrix calculations [33], the latter are included one configuration at a time to ensure completeness of the total trial wave function and to compensate for orthogonality constraints imposed on the continuum orbitals. The use of nonorthogonal one-electron radial functions in the BSR method, on the other hand, allows us to avoid these configurations for compensating orthogonality restrictions.

In the present calculations, the bound channels χ_i were only used for a more accurate description of the $2s^22p^4$ and $2s2p^5$ temporary negative-ion states. The $(2s^22p^4)^3P$ state is located very close to the ground state of nitrogen, and hence its position is very sensitive to the balance of correlation corrections in the N-electron target and the $(N+1)$-electron scattering functions. To maintain this balance, the multiconfiguration expansions for the $2s^22p^4$ and $2s2p^5$ states were obtained in an approximation similar to the one we employed for the nitrogen target states. Specifically, we included all single and double excitations from the $2s$ and $2p$ orbitals to the $3l$ and $4l$ ($l = 0$–3) correlated orbitals, but in this case we used a much smaller cutoff parameter of 0.001 (see discussion below).

The maximum interval in our B-spline grid is $0.65a_0$. This is sufficient to cover electron scattering energies up to 200 eV. The BSR-690 collision model contained up to 1704 scattering channels, leading to generalized eigenvalue problems with matrix dimensions up to 120 000 in the B-spline basis. We calculated partial waves for total orbital angular momenta $L \leqslant 25$ numerically. Taking into account the total spin and parity, this leads to 156 partial waves overall. A top-up procedure based on the geometric-series approximation was used to estimate the contribution from higher L values if needed. The calculation for the external region was performed using a parallelized version of the STGF program [34].

III. RESULTS

A. Elastic and momentum-transfer cross sections

Figure 1 shows the angle-integrated cross section for elastic electron scattering from nitrogen atoms in their $(2s^22p^3)^4S^o$ ground state. The cross section exhibits a prominent near-threshold feature related to the lowest $(2s^22p^4)^3P$ term of N^-. The position of this resonance is very sensitive to the approximation used, and hence experimental work in this energy regime would be highly desirable. Overall, the N^- system and low-energy e-N scattering still remains relatively unexplored by experiment. Direct measurements of the low-energy electron cross section for atomic nitrogen were carried out by Neynaber *et al.* [35]. They employed a crossed-beam setup and reported the grand-total cross section as a function of electron energy from 1.6 to 10 eV. The absolute values were calculated based on the well-known molecular nitrogen cross sections and the ratio of atomic and molecular species in the beam. The reported cross section showed no resonance features

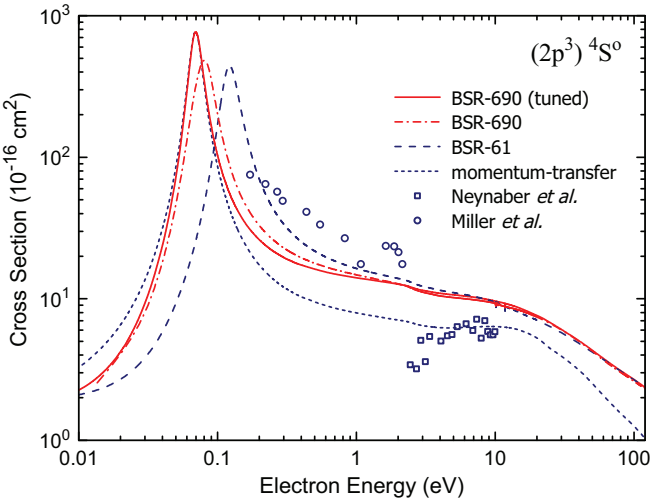

FIG. 1. (Color online) Cross section for elastic electron scattering from nitrogen atoms in their $(2s^22p^3)^4S^o$ ground state. The present results in the BSR-690, BSR-61, and BSR-690 (tuned; see text for details) models are compared with the experimental data of Neynaber *et al.* [35] and Miller *et al.* [36]. Also shown is the momentum-transfer cross section.

and are considerably smaller than all available theoretical predictions.

An experimental indication for a low-energy resonance was provided by Miller *et al.* [36]. Their scattering measurements showed an increasing cross section when reducing the incident energy below 1 eV, which is consistent with the existence of a low-energy shape resonance. These results, however, were not published in detail, and the authors themselves report considerable experimental difficulties. More direct evidence for the ^3P shape resonance originates from the study of the dissociative attachment process by Mazeau *et al.* [4]. By detecting the electrons emitted from N^- ions, the lowest ^3P state of N^- was determined to lie very close to the elastic threshold, just 70 meV above the ground state of neutral atomic nitrogen.

The theoretical position of this resonance is highly sensitive to correlation effects in the model and hence is very difficult to calculate accurately. Some of the most intensive direct atomic-structure calculations for the N^- ground state were undertaken by Wijesundera and Parpia [37]. They employed the multiconfiguration Dirac–Fock (MCDF) method and reported an electron affinity of the N^- system of approximately −181 meV, i.e., corresponding to an unbound state. There were also numerous early attempts to describe this resonance in the framework of collision theory (see, for example, the references in the review by Buckman and Clark [38]).

The apparently-most-successful theoretical prediction of this resonance was provided by Burke *et al.* [5]. They employed a six-state *R*-matrix model, in which they included the three terms of the $2s^22p^3$ ground-state configuration plus three polarized pseudostates that were constructed to provide the full dipole polarizability of the $(2p^3)^4S^o$ ground state. Their values for the position and width, $E = 62$ meV and $\Gamma = 13$ meV, agree very well with the experimental values of Mazeau *et al.* [4]. However, a subsequent similar calculation by the same group [6] with two additional $2s2p^4$ states shifted the resonance below threshold, indicating that the early calculations were not sufficiently converged with respect to target states retained in the close-coupling expansion. A further *ab initio* attempt to describe the ^3P resonance was undertaken by Ramsbottom and Bell [7]. They additionally included four polarized pseudostates determined to represent the polarizabilities of *all* three terms of the ground-state configuration, as well as short-range correlation effects. These calculations, however, did not produce a low-energy ^3P resonant feature either, and the cross section was ultimately calculated by shifting the $(2s^22p^4)^3P$ channel energy in such a way that theory and experiment were in accord with regard to the resonance position. This is a classic example of the difficult balancing act in accounting for correlations in the N-electron-target and the $(N+1)$-electron-collision problems (see also Ref. [39] for a detailed study of an even simpler system: e-Mg collisions).

As seen from Table III, both our BSR-61 and BSR-690 models provide a reasonably accurate description of the ^3P resonance in comparison with the experimental result [4]. Not surprisingly, the BSR-690 calculations predict a lower resonance position and hence a narrower and higher maximum, reflecting the typical convergence pattern of the close-coupling expansion. The position of the resonance, however, is still a little higher than the experimental value. As seen from Fig. 1, the cross section at such low energies depends critically on the resonance position. In order to provide even more accurate cross sections for possible plasma applications, we then "fine tuned" the resonance position to reproduce the experimental result. The position of the resonance in the present calculations predominantly depends on the $(2s^22p^4)^3P$ "perturber" expansion in the close-coupling equations (2). By gradually increasing this expansion we were able to reach the experimental position for this resonance (see Table III). The cross section reaches a peak value of 775×10^{-16} cm^2, thereby considerably exceeding the values at all other energies.

TABLE III. Energies and widths of the three terms with the $2s^22p^4$ configuration in N^-. The energies are given in eV relative to the $(2s^22p^3)^4S^o$ ground state of neutral nitrogen.

Term	Energy (eV)	Width (meV)	Comments
^3P	0.070 (20)	16 (5)	Expt. [4]
	0.181		MCDF [37]
	0.062	13	RM-pol. [5]
	0.122	36	BSR-61
	0.081	24	BSR-690
	0.069	16	BSR-690 (tuned)
^1D	1.40 (10)		Expt. [40]
	1.513		MCHF [41]
	1.34		Extrapolation [42]
	1.406		BSR-61
	1.403		BSR-690
^1S	2.78		Extrapolation [42]
	2.903		MCHF [41]
	2.742		BSR-61
	2.732		BSR-690

Table III also presents the energies for the ^1D and ^1S terms of the $N^-(2s^22p^4)$ configuration. The properties of these negative-ion states are of considerable importance for the application of accelerator mass spectrometry to the measurement of the ^{14}C content of materials [43]. Experimental evidence for the formation of $N^-(^1D)$ states in ion-surface collisions was demonstrated by Müller *et al.* [40]. The position of the ^1D feature was determined to be 1.4 eV above the $^4S^o$ ground state of neutral nitrogen. No indication for the formation of a $(2s^22p^4)^1S$ temporary negative-ion state was found in any of the experiments carried out so far, but existing calculations indicate that the ^1S term is bound to the $(2s^22p^3)^2P^o$ state of neutral nitrogen by at least 0.5 eV. In this case, both the ^1D and ^1S terms are metastable against Coulomb autodetachment. They can only decay to the elastic channel via magnetic interactions for the following reasons: The $2p^3(^4S^o)\varepsilon l$ continuum can have only a quintet or triplet total spin. In a nonrelativistic LS-coupling framework, therefore, neither the ^1D nor the ^1S state could autodetach into the N $(2p^3)^4S^o$ channel. Furthermore, $2s^22p^3(^2D^o)\varepsilon l$ cannot couple to a state of overall ^1S symmetry.

We define the energies of these terms through the position of the lowest R-matrix poles in the corresponding partial waves. Our energy of 1.406 eV for the ^1D temporary state is in good agreement with the experimental value, and we expect a similar accuracy for the position of the ^1S term. Some

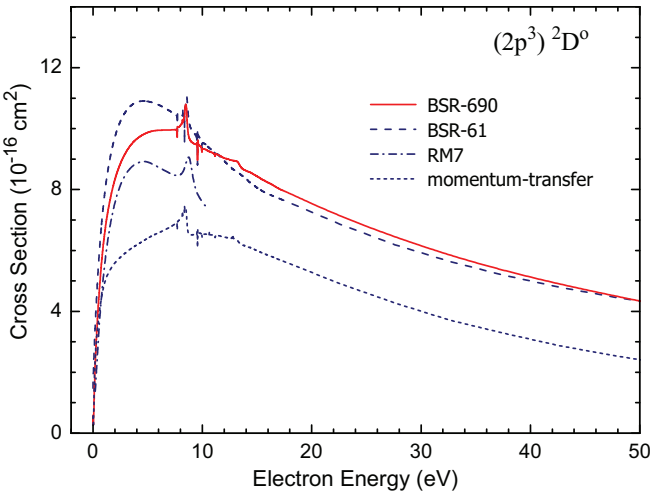

FIG. 2. (Color online) Cross section for elastic electron scattering from nitrogen atoms in the metastable $(2s^2 2p^3)^2 D^o$ state. The present BSR-690 results are compared with those from a BSR-61 model and a seven-state R-matrix (RM7) calculation [7]. Also shown is the momentum-transfer cross section.

selected results from previous calculations are also presented in Table III for comparison. Thomas and Nesbet [42] published predictions based on a quadratic extrapolation of the term energies corresponding to the $2s^2 2p^4$ configurations in O, F^+, and Ne^{++}. Furthermore, Cowan and Froese Fischer [41] applied systematic MCHF procedures to the study of the electron affinities and lifetimes for the ^1D and ^1S states. While their estimates somewhat disagree with our values, the differences never exceed 0.1 eV.

Elastic cross sections for electron scattering from the metastable states of atomic nitrogen are presented in Figs. 2 and 3 for the $(2s^2 2p^3)^2 D^o$ and $(2s^2 2p^3)^2 P^o$ states, respectively.

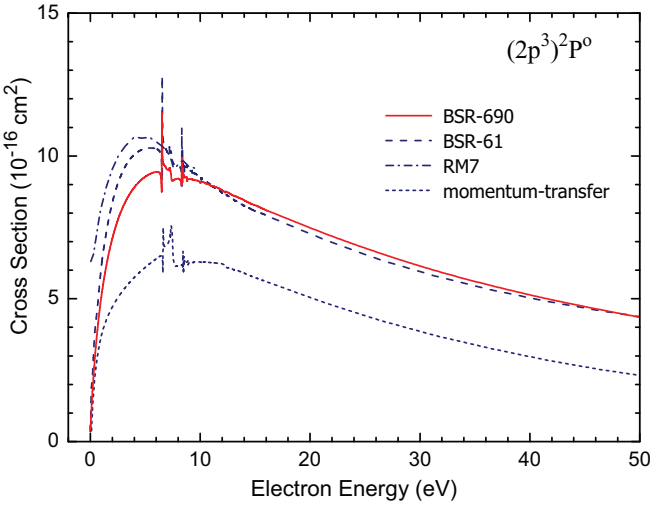

FIG. 3. (Color online) Cross section for elastic electron scattering from nitrogen atoms in the metastable $(2s^2 2p^3)^2 P^o$ state. The present BSR-690 results are compared with those from a BSR-61 model and a seven-state R-matrix (RM7) [7]. Also shown is the momentum-transfer cross section.

We compare the present results from the BSR-61 and BSR-690 models with the seven-state R-matrix calculations (RM7) by Ramsbottom and Bell [7]. All calculations predict a similar energy dependence with a maximum around 5 eV. Including the continuum pseudostates in the BSR-690 model decreases the maximum values by up to 10% in comparison to the BSR-61 calculations. The BSR-690 cross sections considerably exceed the RM7 results for the $^2D^o$ state, while they are noticeably smaller for the $^2P^o$ state. For clarity, we only compare with the most recent R-matrix calculations [7]. Other results from different models were discussed in Ref. [7] and show rather scattered absolute values, some considerably exceeding the present results in the peak. This is likely due to the fact that a much better description of the polarizability of the $^2D^o$ and $^2P^o$ metastable states was included in the present work and also in Ref. [7]. Our calculations predict polarizabilities of $7.32a_0^3$, $7.69a_0^3$, and $8.22a_0^3$ for the $^4S^o$, $^2D^o$, and $^2P^o$ terms, respectively. For the $^4S^o$ ground state, the polarizability closely agrees with the experimental value of $7.6a_0^3 \pm 0.4a_0^3$ [44].

The momentum-transfer cross sections shown in Figs. 1–3 are all significantly smaller than the corresponding elastic cross sections. The notable exception is the ^3P resonance region for scattering from the $^4S^o$ ground state, where the two cross sections are very close to each other. Clearly, if momentum-transfer cross sections are needed in plasma applications, they should not simply be replaced by elastic cross sections if the former are not available.

B. Excitation cross sections

Cross sections as a function of energy for the most important transitions from the ground state and the metastable states are presented in Figs. 4–6. To check the convergence of the results, we compare the predictions from four BSR models, gradually increasing the number of target states from 21 to 690. A previous comparison with early calculations (which contained less target states) was presented in Ref. [12].

Let us first consider a few selected transitions from the ground state, which are presented in Fig. 4. For the spin-forbidden exchange transition $(2s^2 2p^3)^4 S^o$-$(2s^2 2p^3)^2 D^o$, excellent agreement is obtained between the results from all models presented. Convergence is hence evident over a wide range of electron-impact energies. We conclude that the theoretical cross section for this important transition has now likely been established to an accuracy of a few percent. The agreement between the calculated cross sections and experiment [10] is also excellent at all incident-electron energies except for 5 eV, which is the lowest energy for which the measurement was carried out. Despite the rather large uncertainties in the experimental cross sections, the good agreement between experiment and theory supports the suggested accuracy of the theoretical cross sections.

Close agreement between all BSR calculations is also obtained for the other important exchange transition, $(2s^2 2p^3)^4 S^o$-$(2s^2 2p^3)^2 D^o$. The cross sections rise sharply close to the threshold and exhibit a broad peak around 7 eV in all calculations. There is also a noticeable resonance structure in the energy region 10–13 eV before the cross-section values smoothly decrease at higher energies. The dominant resonance

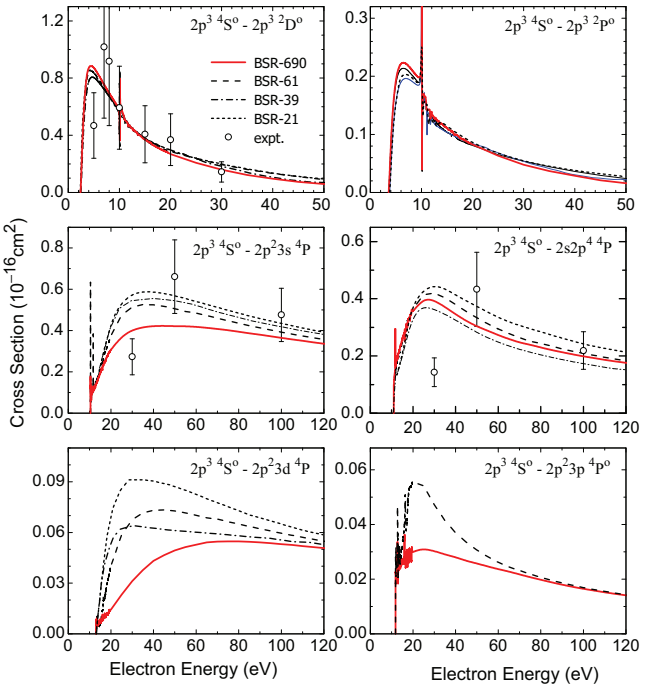

FIG. 4. (Color online) Cross sections, as function of collision energy, for electron-impact excitation of the most important transitions from the $(2s^2 2p^3)^4S^o$ ground state of atomic nitrogen. The final states are listed in the various panels. Unless listed explicitly as $2s$, the inner-shell configuration is $1s^2 2s^2$. The present BSR-696 and BSR-61 results are compared with those from the previous BSR-39 and BSR-21 calculations by Tayal and Zatsarinny [12]. Also shown are various sets of experimental data [8–10].

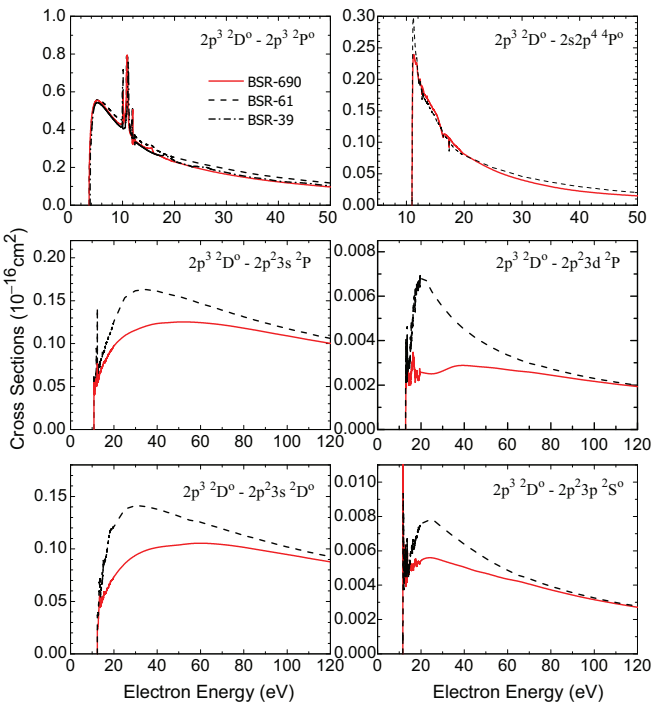

FIG. 5. (Color online) Cross sections as function of collision energy for electron-impact excitation of the most important transitions from the $(2s^2 2p^3)^2D^o$ metastable state of atomic nitrogen. The final states are listed in the various panels.

is due to the $N^-(2s^2 2p^2 3s^2)^3P$ resonance around 10 eV. The cross sections for the $^4S^o$-$^2P^o$ transition are approximately one third of the cross sections of the $^4S^o$-$^2D^o$ transition. We suggest that they, too, have been established to an accuracy of a few percent, even though no experimental results for this transition are available to compare with theory.

The convergence for the dipole transitions with regard to the number of states in the close-coupling expansion is not as fast as for the exchange transitions considered above. A strong influence of the target continuum is found, for example, for the dipole-allowed transition to the $(2s^2 2p^2 3s)^4P$ state, where the cross section in the maximum decreases by ≈30% in the BSR-690 model compared to the other calculations. The absolute measured cross sections of Doering and Goembel [8] for this transition at 30, 50, and 100 eV agree reasonably well with the calculations at 100 eV and with the BSR-690 result at 30 eV, but they considerably exceed the BSR-690 predictions at 50 eV. Given the well-known trends associated with the inclusion of additional pseudostates, we believe that the BSR-690 model produces the most reliable results, and hence that the agreement between experiment and the other theories within the experimental error bars is accidental.

For the $(2s^2 2p^3)^4S^o$-$(2s 2p^4)^4P$ transition, the inclusion of the continuum pseudostates in the BSR-39 and BSR-690 models leads to a 10% to 20% reduction in the predicted cross sections over a wide range of electron energies. It should be noted that part of the difference between the cross sections from the 39-state and 690-state calculations may be due to the improved target wave functions in our 690-state model. Absolute measured cross sections were again published by Doering and Goembel [9] at 30, 50, and 100 eV. We see good agreement with experiment for 100 eV, decent agreement within the error bars for 50 eV, and a large difference for 30 eV. We cannot comment on potential experimental issues, but we would be surprised if our predictions were inaccurate to such a large extent.

A much stronger influence of coupling to the target continuum is seen for the transition to the $(2s^2 2p^2 3d)^4P$ state. This transition is much weaker than those considered before, and hence channel-coupling effects are expected to be more important. The final example presented in Fig. 4 concerns the quadrupole transition to the $(2s^2 2p^2 3p)^4P^o$ state. Comparison between the BSR-61 and BSR-690 results once again shows a strong influence of the target continuum for this transition, resulting in a decrease of the peak value by almost a factor of two.

The cross sections for transitions from the metastable $(2s^2 2p^3)^2D^o$ and $(2s^2 2p^3)^2P^o$ states shown in Figs. 5 and 6 exhibit principal features similar to those of the transitions from the ground state. Here we mainly compare the results from the present BSR-61 and BSR-690 models, thereby concentrating on the influence of coupling to the target continuum. Only for the dipole-forbidden $(2s^2 2p^3)^2D^o$-$(2s^2 2p^3)^2P^o$ transition do we have cross sections from previous calculations available for comparison. We first note that the BSR-39 cross sections for this transition were presented incorrectly in Fig. 5 of Ref. [12], but the correct BSR-39 cross sections are shown in Fig. 5 here.

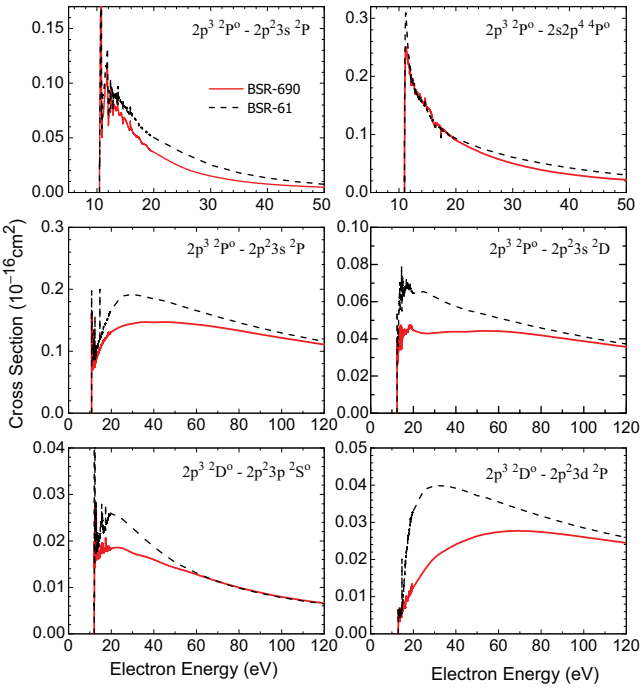

FIG. 6. (Color online) Cross sections as function of collision energy for electron-impact excitation of the most important transitions from the $(2s^2 2p^3)^2P^o$ metastable state of atomic nitrogen. The final states are listed in the various panels.

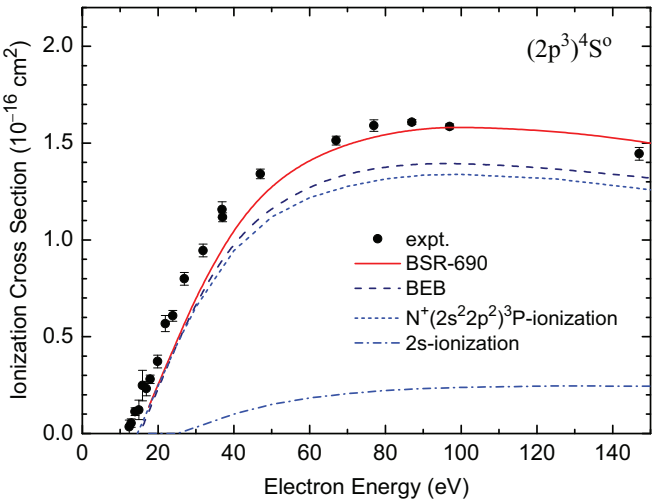

FIG. 7. (Color online) Cross sections for electron-impact ionization of atomic nitrogen from the $(2s^2 2p^3)^4S^o$ ground state. The present BSR-690 results are compared with the BEB predictions of Kim and Desclaux [14] and the experimental data of Brook *et al.* [13]. Also shown are the individual contributions to the signal from $2p$ ionization leading to the final ionic state $(2s^2 2p^2)^3P$ and from $2s$ ionization.

Now all scattering models yield very similar results, indicating that the theoretical cross sections are well converged and are likely accurate to within a few percent.

There is a noticeable resonance structure at electron energies between 10 and 13 eV (note that the electron energies are given relative to the ground state). The dominant resonance corresponds to the $N^-(2s2p^5)^3P$ temporary negative-ion state around 11 eV, which is consistent with our previous more-detailed resonance analysis given in Ref. [12]. It is worth mentioning that this resonance has no effect on the $^4S^o$-$^2D^o$ and $^4S^o$-$^2P^o$ excitation cross section considered above, since the $^4S^o$ ground state cannot couple with a continuum orbital to form a ^3P scattering state. As discussed in Ref. [7], the position of this resonance is very sensitive to the target expansions used, and hence early calculations provided very different resonance positions for this case.

Close agreement between the BSR-61 and BSR-690 results is also found for the exchange transitions $(2s^2 2p^3)^2D^o$-$(2s2p^4)^4P^o$ and $(2s^2 2p^3)^2P^o$-$(2s2p^4)^4P^o$, respectively. It appears that the target continuum only has a minor influence on the exchange transitions in the e-N collision system or for other transitions that are dominated by short-range interactions.

For the dipole-allowed one-electron $2p$-$3s$ and $2p$-$3d$ promotions as well as for the quadrupole $2p$-$3p$ transition presented in Figs. 5 and 6, the BSR-690 cross sections are considerably lower than the BSR-61 results at intermediate energies. The corrections range from 10% to 50%, with the largest effect seen for the $2p$-$3d$ transition. The present findings regarding the influence of coupling to the target continuum in electron collisions with atomic nitrogen agree well with the trend seen in recent calculations for electron scattering from C [17], F [45], and Ne [16], all atoms with a partially or fully filled outer $2p$ subshell. For all these atoms the target-continuum corrections are significant and increase with the occupation of that p subshell.

C. Ionization cross sections

Figure 7 exhibits the cross section for electron-impact ionization of atomic nitrogen from the $^4S^o$ ground state. The present BSR-690 results were obtained by adding the excitation cross sections for all target states above the first ionic ground state. That includes the direct contribution from the continuum pseudostates and an appropriate portion of the excitation cross sections of quasidiscrete states in the continuum; so-called excitation autoionization. In nitrogen, the dominant contribution from excitation-autoionization is expected from excitation of the $2s2p^4$ states, due to the strong $2s$-$2p$ one-electron transition. The $2s2p^4$ configuration can result in ^4P, ^2P, ^2D, and ^2S terms. Since the $(2s2p^4)^4P$ state lies below the ionization threshold, however, and the excitation of this state is dipole-allowed from the $^4S^o$ ground state, we do not expect a significant contribution to the total ionization from excitation autoionization of just the $2s2p^4$ doublet states.

As seen from Fig. 7, our fully *ab initio* BSR results are in overall good agreement with the experimental data of Brook *et al.* [13], although the theoretical results lie systematically below experiment at lower energies. This may be related to a still relatively low density of continuum pseudostates in this energy regime. On the other hand, Brook *et al.* mention some uncertainty in the value of the experimental contact potential, which would affect the absolute energy scale. Note that the ionization potential for atomic nitrogen is about 14.5 eV [27]. Hence a slight shift of the experimental data in Fig. 7 to the right may be appropriate.

The semi-empirical BEB predictions of Kim and Desclaux [14] follow the BSR results at low energies, but then underestimate the ionization cross sections by ≈15% around the maximum. In order to explain this discrepancy, Kim and Desclaux suggested a large admixture (up to 30%) of metastable nitrogen atoms in the experiment. Our results, however, do not require such an assumption. Other calculations for electron-impact ionization of nitrogen atoms have been reported in the literature. They were carried out in variants of the Born approximation and were discussed by Brook *et al.* As expected from the general features of the Born theory, all these calculations considerably overestimate the ionization cross section at maximum.

While the semi-empirical BEB predictions for the total ionization cross section might still be considered to be in reasonable agreement with the present results, we note that they predict entirely different partial contributions from the residual ionic states. In order to obtain ionization cross sections from the BSR with pseudostates approach, we project the continuum pseudostates onto the corresponding ionic states included in the target expansion (1) and then use these projections to estimate the respective partial cross sections.

The lowest term of N^+ corresponds to $(2s^2 2p^2)^3P$, and the ion has two metastable terms, $(2s^2 2p^2)^1D$ and ^1S. We found that ionization-excitation processes to the N^+ metastable states are negligibly small (less than 1%), and hence the total ionization cross section is mainly defined by $2p$ ionization to the ionic $(2s^2 2p^2)^3P$ ground state, plus a noticeable contribution from ionization of a $2s$ electron. The corresponding partial cross sections are depicted in Fig. 7. In the BEB model, final-state data are not used explicitly, although indirectly via the corresponding ionization energy. Most experiments for total ionization cross sections do not distinguish the resulting ionic states, and hence theory must sum over these final states, which are often metastable.

Kim and Desclaux [14] suggested modifying the BEB model when the resulting ions have more than one LS term, where L and S are the total orbital and spin angular momenta. They assumed that the ratios of the ions in different final states of the same electronic configuration of the ion are close to the corresponding statistical ratios. In the present case of atomic nitrogen, therefore, the BEB calculations contain three steps: (i) calculate the BEB ionization cross sections for the three ionic terms ^3P, ^1D, and ^1S with appropriate ionization energies; (ii) weight the cross sections for these ionic states by 9/15, 5/15, and 1/15, respectively; (iii) sum the weighted cross sections to obtain the total ionization cross section. Since the ionization energies are similar for the three final ionic states, this procedure leads to relatively small corrections to the total ionization cross section compared with straightforward calculations without the LS decomposition. However, this statistical-ratio method produces very different partial cross sections from the present *ab initio* calculations discussed above.

Ionization cross sections from the metastable states of nitrogen are presented in Figs. 8 and 9. Due to the lower ionization energies, these cross sections are noticeably larger than the ground-state cross sections. We again note reasonable agreement with the BEB predictions, but their decomposition according to the final ionic states and excitation-autoionization

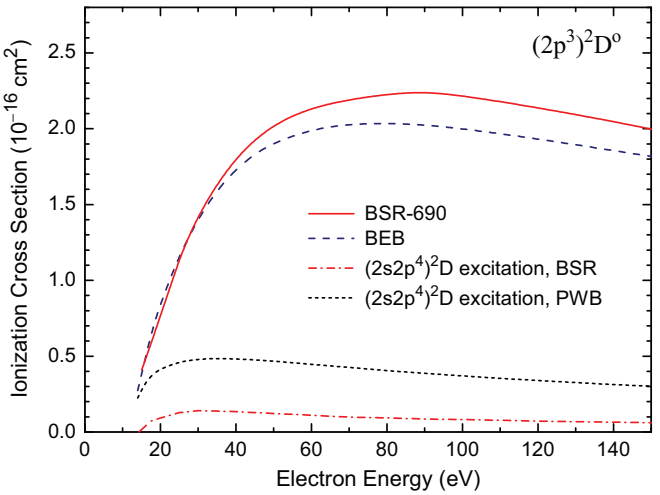

FIG. 8. (Color online) Cross sections for electron-impact ionization of atomic nitrogen from the metastable $(2s^2 2p^3)^2D^o$ state. The present BSR-690 results are compared with the BEB predictions of Kim and Desclaux [14]. Also shown are the $(2s2p^4)^2D$ excitation cross sections, which provide the main contribution to the autoionization-excitation process (see text for details).

contribution are very different from those obtained from the present *ab initio* numerical calculations.

Let us first consider the excitation-autoionization contribution from the $2s2p^4$ states. The ^2S and ^2P terms were found to lose their distinct identities through strong mixing with either the $2s^2 2p^2 ns$ and $2s^2 2p^2 nd$ series or with the underlying continuum background, and only the ^2D term has been observed at 15.03 eV above the ground state [27]. This state was chosen by Kim and Desclaux as the only important state for the excitation-autoionization in nitrogen atoms, and they predict a large contribution from excitation autoionization

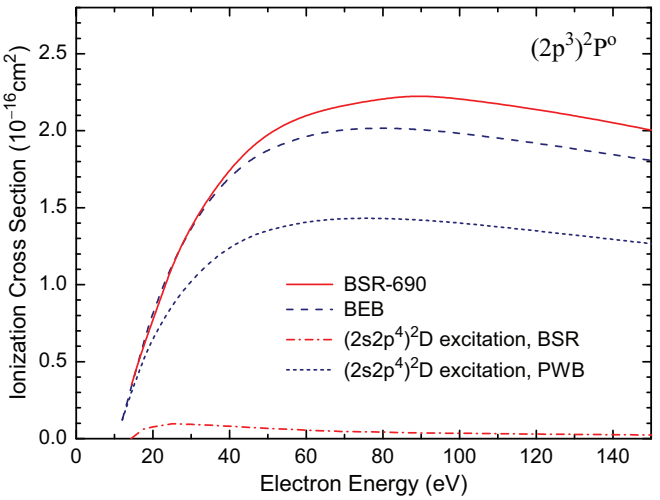

FIG. 9. (Color online) Cross sections for electron-impact ionization of atomic nitrogen from the metastable $(2s^2 2p^3)^2P^o$ state. The present BSR-690 results are compared with the BEB predictions of Kim and Desclaux [14]. Also shown are the $(2s2p^4)^2D$ excitation cross sections, which provide the main contribution to the autoionization-excitation process (see text for details).

of the $(2s2p^4)^2D$ state. For example, this contribution becomes dominant for ionization of the $(2p^3)^2P$ metastable state shown in Fig. 9.

The corresponding excitation cross section was obtained by Kim and Desclaux in the plane-wave Born (PWB) approximation. The present BSR calculations, on the other hand, yield a much smaller contribution from excitation autoionization. The main reason for the discrepancy lies in the different description of the $(2s2p^4)^2D$ state. Kim and Desclaux used oscillator strengths and wave functions from MCDF calculations, and their f values are about a factor of five larger than our values presented in Table II. Note that our oscillator strengths are in close agreement with the values calculated by Hibbert *et al.* [46]. (A direct comparison is difficult due to the fine-structure-resolved values in the intermediate coupling scheme.) Using the f values of Hibbert *et al.*, or our values, would drastically reduce the PWB excitation-autoionization cross sections and bring them into much better agreement with the present BSR calculations.

Since the total ionization cross sections from the BSR-690 and BEB calculations agree within 20%, the large relative contribution from excitation autoionization in the BEB calculations makes the relative contribution of direct ionization much smaller than in the present results. Finally, we note that the relative decomposition among the final ionic states for ionization of the metastable ^2D and ^2P states was found to be close to the statistical ratios used in the BEB calculations.

D. Grand-total cross sections from ground and metastable states

Figures 10–12 show our present results in a form that might be useful for many plasma applications. Specifically, we show how the grand-total cross section, which is composed of the elastic contribution, all inelastic-excitation processes summed up, ionization, and—for the excited metastable initial states $(2p^3)^2D^o$ and $(2p^3)^2P^o$—*superelastic deexcitation*. While the elastic cross section provides the largest contribution over the energy range shown, ionization also contributes substantially at energies above 50 eV. Ionization is even more important for the metastable excited states, reaching 40% of the grand-total cross section at 100 eV. Excitation processes, on the other hand, overall represent less than 10% of the grand-total cross section. Deexcitation of the $^2D^o$ metastable state to the $^4S^o$ ground state exhibits the well-known exchange character of spin-changing transitions and is almost negligible in comparison to the other processes. Deexcitation of the $^2P^o$ metastable state, in contrast, is more important and shows a prominent narrow peak near threshold. This fact could be important if the amount of metastable atoms in the system is significant.

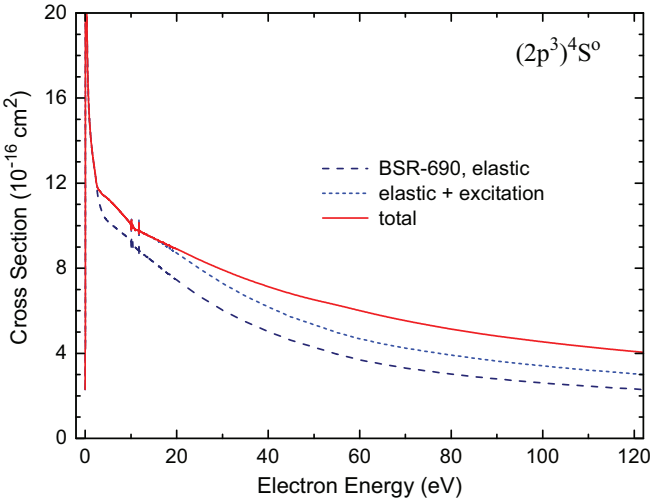

FIG. 10. (Color online) Elastic, elastic + excitation, and grand-total cross section for electron collisions with atomic nitrogen in the $(2s^22p^3)^4S^o$ ground state.

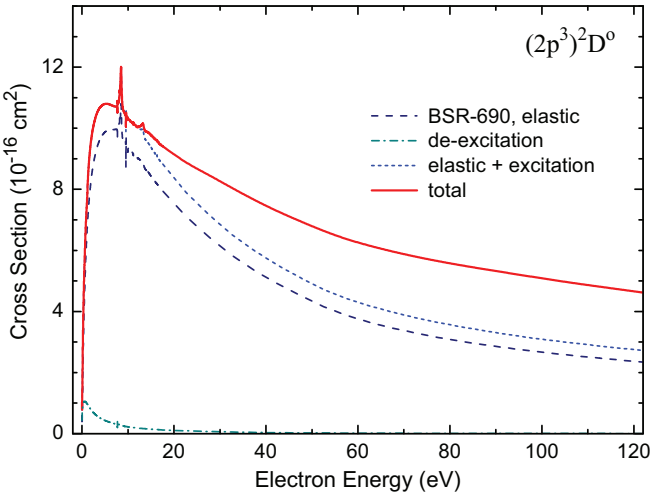

FIG. 11. (Color online) Elastic, elastic + excitation, elastic + excitation + ionization, and grand-total cross section for electron collisions with atomic nitrogen in the $(2s^22p^3)^2D^o$ metastable state. In this case, the grand-total cross section also contains deexcitation through superelastic scattering.

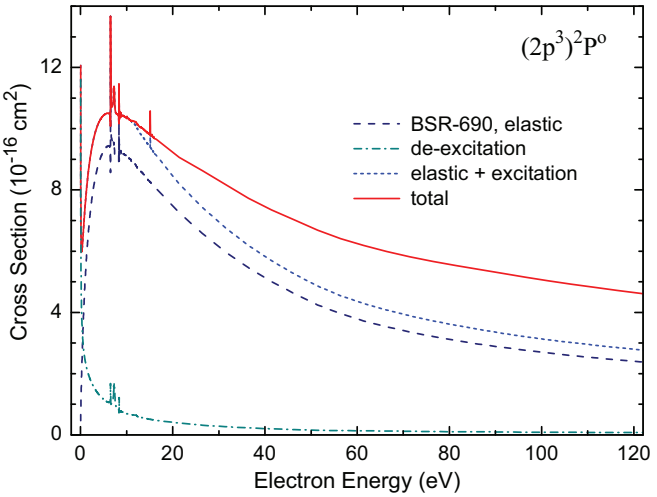

FIG. 12. (Color online) Elastic, elastic + excitation, elastic + excitation + ionization, and grand-total cross sections for electron collisions with atomic nitrogen in the $(2s^22p^3)^2P^o$ metastable state. In this case, the grand-total cross section also contains deexcitation through superelastic scattering.

IV. SUMMARY AND CONCLUSIONS

We presented a revised set of cross sections for elastic scattering as well as electron-induced excitation, deexcitation, and ionization of atomic nitrogen initially in its ground or metastable state. The calculations were performed with the B-spline R-matrix method, where a B-spline basis is employed for the representation of the continuum functions and the use of nonorthogonal orbital sets allows for high flexibility, and hence accuracy, in the construction of the target wave functions. The latter can be independently optimized for each state of interest.

Compared to our previous BSR calculation [12], the target description was further improved in the current work by combining the strengths of the MCHF and BSR approaches. Furthermore, a large number of pseudostates was included in the close-coupling expansion. These pseudostates allow for the treatment of two important features, namely: (i) accounting for the influence of coupling to the target ionization continuum (and high-lying Rydberg states) on transitions between the discrete states that are most interesting for plasma modeling; and (ii) *ab initio* calculations of the ionization cross section. In our scattering calculations we attempted to include the most important physical effects, including short-range correlation in the target states and long-range polarization effects in the scattering system. This allowed us to obtain an accurate representation of the elastic cross section at low energies, where the scattering exhibits a prominent near-threshold resonance related to the $(2s^2 2p^4)^3P$ term of N^-.

We used several collision models to check the convergence of the predicted cross sections with respect to the number of target states included in the close-coupling expansion. Comparison of these results with each other as well as the available experimental data leads us to conclude that the excitation cross sections for transitions between all terms of the $2s^2 2p^3$ ground-state configuration have now been established to an accuracy of a few percent. Very accurate results are also expected for the strong and important transitions to the $(2s2p^4)^4P$ state. For these transitions coupling to the continuum was found to only have a minor influence on the results.

The transitions to the $2s^2 2p^3 nl$ valence states were found to be strongly affected by coupling to the target continuum. Compared with previous predictions, the corresponding corrections reach a factor of two for some dipole and quadrupole transitions, especially for transitions involving $2p$-$3d$ electron promotion. This extreme sensitivity seems to be a general trend in atoms with outer p shells; it agrees well with our previous findings in calculations for carbon, fluorine, and neon atoms. As explained in a recent paper [47], the principal physical reason for this result is the stability of the elastic and grand-total cross sections against changes in the theoretical models. While this also implies stability of the *combined* cross section for excitation plus ionization, the *distribution* between the two possibilities can vary substantially. Basically, if there are not enough (or no) pseudostates with energies above the ionization threshold retained in the close-coupling expansion, then excitation will take up too much (or even all) flux into the inelastic channels.

We used the largest close-coupling expansions that we could handle with modern computational resources. Our experience with such calculations leads us to suggest that the present results are by far the most accurate available today and hence should be used for modeling purposes as the preferred set of *ab initio* term-resolved data for this collision system.

Our extensive R-matrix-with-pseudostates model also allowed us to carry out nonperturbative calculations of the ionization cross sections from the ground and metastable states of atomic nitrogen. Close agreement was obtained with the available experimental data, and reasonable agreement for the total ionization cross section also with BEB predictions. However, the final ionic-state population for ionization from the ground state was found to differ considerably from the statistical assumption made in the BEB calculations. The excitation-autoionization contribution for the metastable-state ionization also differs considerably from the BEB estimates.

Electronic files with the current results, for electron energies up to 100 eV, are available from the authors upon request. The dataset includes the complete set of excitation cross sections for all transitions between the first 21 states of atomic nitrogen as well as elastic, momentum-transfer, and ionization cross sections for the ground and metastable states.

ACKNOWLEDGMENTS

This work was supported by the United States National Science Foundation under Grants No. PHY-1068140 and No. PHY-1212450, and by the XSEDE allocation No. PHY-090031. One of us (K.B.) would like to thank Professor M. J. Brunger and Dr. L. Campbell for stimulating discussions and helpful comments on the manuscript, and Flinders University for their hospitality and financial support of his visit during which part of this work was performed.

[1] C. O. Laux, T. G. Spence, C. H. Kruger, and R. N. Zare, Plasma Sources Sci. Technol. **12**, 125 (2003).
[2] J. Shoeb and M. J. Kushner, J. Vac. Sci. Technol., A **29**, 051305 (2011).
[3] N. Yu. Babaeva and M. J. Kushner, Plasma Sources Sci. Technol. **23**, 015007 (2014).
[4] J. Mazeau, F. Gresteau, R. I. Hall, and A. Huetz, J. Phys. B: At. Mol. Phys. **11**, L557 (1978).
[5] P. G. Burke, K. A. Berrington, M. Le Dourneuf, and Vo Ky Lan, J. Phys. B: At. Mol. Phys. **7**, L531 (1974).
[6] K. A. Berrington, P. G. Burke, and W. D. Robb, J. Phys. B: At. Mol. Phys. **8**, 2500 (1975).
[7] C. A. Ramsbottom and K. L. Bell, Phys. Scr. **50**, 666 (1994).
[8] J. P. Doering and L. Goembel, Geophys. Res. **96**, 16021 (1991).
[9] J. P. Doering and L. Goembel, Geophys. Res. **97**, 4295 (1992).
[10] J. Yang and J. P. Doering, Geophys. Res. **101**, 21765 (1996).
[11] S. S. Tayal and C. A. Beatty, Phys. Rev. A **59**, 3622 (1999).
[12] S. S. Tayal and O. Zatsarinny, J. Phys. B: At., Mol. Opt. Phys. **38**, 3631 (2005).

[13] E. Brook, M. F. A. Harrison, and A. C. H. Smith, J. Phys. B: At. Mol. Phys. **11**, 3115 (1978).
[14] Y.-K. Kim and J.-P. Desclaux, Phys. Rev. A **66**, 012708 (2002).
[15] O. Zatsarinny and K. Bartschat, Phys. Rev. A **85**, 062710 (2012).
[16] O. Zatsarinny and K. Bartschat, Phys. Rev. A **86**, 022717 (2012).
[17] Y. Wang, O. Zatsarinny, and K. Bartschat, Phys. Rev. A **87**, 012704 (2013).
[18] O. Zatsarinny, Comput. Phys. Commun. **174**, 273 (2006).
[19] I. Bray and A. T. Stelbovics, Phys. Rev. A **46**, 6995 (1992).
[20] K. Bartschat, E. T. Hudson, M. P. Scott, P. G. Burke, and V. M. Burke, J. Phys. B: At., Mol. Opt. Phys. **29**, 115 (1996).
[21] O. Zatsarinny and K. Bartschat, Phys. Rev. Lett. **107**, 023203 (2011).
[22] O. Zatsarinny and K. Bartschat, Phys. Rev. A **85**, 062709 (2012).
[23] K. A. Berrington, W. B. Eissner, and P. H. Norrington, Comput. Phys. Commun. **92**, 290 (1995).
[24] N. R. Badnell, http://amdpp.phys.strath.ac.uk/UK_RmaX/codes.html (2014).
[25] O. Zatsarinny and C. Froese Fischer, Comput. Phys. Commun. **180**, 2041 (2009).
[26] C. Froese Fischer, G. Tachiev, G. Gaigalas, and M. R. Godefroid, Comput. Phys. Commun. **176**, 559 (2007).
[27] A. Kramida, Yu. Ralchenko, J. Reader, and NIST ASD Team, *NIST Atomic Spectra Database* (ver. 5.1), http://physics.nist.gov/asd (2013).
[28] C. Goldbach, M. Martin, G. Nollez, P. Plomdeur, and J.-P. Zimmermann, Astron. Astrophys. **161**, 47 (1986).
[29] H. W. Smith, J. Bromander, L. J. Curtis, and R. Buchta, Phys. Scr. **2**, 211 (1970).
[30] P. M. Lugger, D. G. York, T. Blanchard, and D. C. Morton, Astrophys. J. **224**, 1059 (1978).
[31] C. Goldbach, T. Luedtke, M. Martin, and G. Nollez, Astron. Astrophys. **266**, 605 (1992).
[32] C. Goldbach and G. Nollez, Astron. Astrophys. **201**, 189 (1988).
[33] P. G. Burke, *R-Matrix Theory of Atomic Collisions* (Springer-Verlag, Berlin, Heidelberg, 2011).
[34] N. Badnell, J. Phys. B: At., Mol. Opt. Phys. **32**, 5583 (1999); see also http://amdpp.phys.strath.ac.uk/UK_RmaX/codes.html
[35] R. H. Neynaber, L. L. Marino, E. W. Rothe, and S. M. Trujillo, Phys. Rev. **129**, 2069 (1963).
[36] T. M. Miller, B. B. Aubrey, P. N. Eisner, and B. Bederson, Bull. Am. Phys. Soc. **15**, 416 (1970).
[37] W. P. Wijesundera and F. A. Parpia, Phys. Rev. A **57**, 3462 (1998).
[38] S. J. Buckman and C. W. Clark, Rev. Mod. Phys. **66**, 539 (1994).
[39] K. Bartschat, O. Zatsarinny, I. Bray, D. V. Fursa, and A. T. Stelbovics, J. Phys. B: At., Mol. Opt. Phys. **37**, 2617 (2004).
[40] H. Müller, D. Gador, F. Wiegershaus, and V. Kempter, J. Phys. B: At., Mol. Opt. Phys. **29**, 715 (1996).
[41] R. D. Cowan, C. Froese Fischer, J. E. Hansen, and V. Kempter, J. Phys. B: At., Mol. Opt. Phys. **30**, 1457 (1997).
[42] L. D. Thomas and R. K. Nesbet, Phys. Rev. A **12**, 2369 (1975).
[43] W. Kutschera, Nucl. Phys. News **3**, 15 (1993).
[44] R. D. Alpher and D. R. White, Phys. Fluids **2**, 153 (1959).
[45] V. Gedeon, S. Gedeon, V. Lazur, E. Nagy, O. Zatsarinny, and K. Bartschat, Phys. Rev. A **89**, 052713 (2014).
[46] A. Hibbert, E. Biemont, M. Godefroid, and N. Vaeck, Astron. Astrophys., Suppl. Ser. **88**, 505 (1991).
[47] O. Zatsarinny, Y. Wang, and K. Bartschat, Phys. Rev. A **89**, 022706 (2014).